Supervisory Model Predictive Control of the Heat Integrated Distillation Column

Meyer, Kristian; Bisgaard, Thomas; Huusom, Jakob Kjøbsted; Abildskov, Jens

Published in:
IFAC-PapersOnLine

Link to article, DOI:
10.1016/j.ifacol.2017.08.1506

Publication date:
2017

Document Version
Publisher's PDF, also known as Version of record

Available online at www.sciencedirect.com

ScienceDirect

IFAC Papers Online CONFERENCE PAPER ARCHIVE

IFAC PapersOnLine 50-1 (2017) 7375–7380

Supervisory Model Predictive Control of the Heat Integrated Distillation Column

Kristian Meyer * **Thomas Bisgaard** * **Jakob K. Huusom** * **Jens Abildskov** *

* *Department of Chemical and Biochemical Engineering, Technical University of Denmark, Søltofts Plads Building 227, DK-2800, Kgs. Lyngby, Denmark (e-mail: ja@kt.dtu.dk).*

Abstract: This paper benchmarks a centralized control system based on model predictive control for the operation of the heat integrated distillation column (HIDiC) against a fully decentralized control system using the most complete column model currently available in the literature. The centralized control system outperforms the decentralized system, because it handles the interactions in the HIDiC process better. The integral absolute error (IAE) is reduced by a factor of 2 and a factor of 4 for control of the top and bottoms compositions, respectively.

Keywords: Control system design, distillation columns, HIDiC, heat integration, predictive control, dynamic systems

1. INTRODUCTION

The heat integrated distillation column (HIDiC) has been shown to be an attractive energy efficient distillation technology that can outperform both the conventional distillation column (CDiC) and the state-of-the-art mechanical vapour recompression column (MVRC) with respect to energy and cost, at least for some energy-intensive separations (Shahandeh et al. (2014)). In the HIDiC (Mah et al. (1977), Figure 1), heat is allowed to be transferred between the two column sections. The desired direction of heat is obtained using a compressor introduced above the feed stage. The liquid from the high pressure section is throttled before entering the low pressure section.

The operation of the HIDiC has been studied extensively in the literature (e.g. Nakaiwa et al. (1998); Schmal et al. (2006); Huang et al. (2007); Liu et al. (2011); Bisgaard et al. (2017)). Strong loop interactions have been reported. Schmal et al. (2006) studied the operation of a HIDiC splitting a propylene/propane mixture, and indicated that a model predictive control (MPC) based scheme would have improved their operational results due to interactions between loops. Recently, Bisgaard et al. (2017) studied optimal operation of the HIDiC for two case studies where benzene/toluene and a multicomponent aromatic mixture was separated. Here, it was also speculated that multivariable control strategies could potentially improve the operation of the HIDiC. As a result of process intensification, the manipulated variables in the HIDiC often affect both the top and bottoms composition with a similar magnitude, making multivariable control strategies potentially attractive for dual-composition control. Here we will test the performance of advanced control strategies for operation of the HIDiC. There are no references (known to us) where such methods have been implemented. An MPC-based supervisory control scheme is compared to a fully decentralized proportional-integral (PI) control scheme for

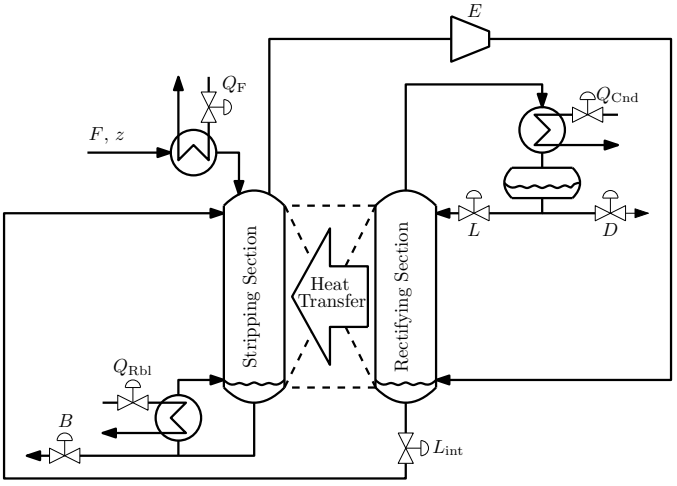

Fig. 1. General conceptual representation of the HIDiC with notation.

HIDiC operation in order to explore potential benefits. The control system consists of a lower level regulatory control layer stabilizing the column and a supervisory control layer that controls both product compositions. In the decentralized system, the best pairings of inputs with outputs is determined using the LACEY procedure (Luyben (2012)). This analysis is consistent with Nakaiwa et al. (1999). They used a simpler model compared to the model used here.

The outline of this paper is as follows. In section 2 the HIDiC model and design is given. In section 3 a fully decentralized control scheme based on PI-control is designed. In section 4 a centralized control system based on supervisory MPC-control is designed and benchmarked against the decentralized control system. Finally concluding remarks are collected in section 5.

10.1016/j.ifacol.2017.08.1506

2. HIDIC MODEL AND DESIGN

The present HIDiC model is adopted from Bisgaard et al. (2015), who presents the model documentation and solution procedure. The model includes dynamic mass and energy balances, varying stage pressures and liquid and vapour hydraulics. The model is currently considered the most complete column model available in the literature. Its dynamic degrees of freedom are given in Figure 1. In order to demonstrate the capabilities of the proposed control structures, a benzene-toluene case study is chosen as this represents the most studied separation in HIDiC literature. Separation specifications (Table 1) are adopted from Nakaiwa et al. (1999), and includes feed characteristics, product purities, number of equilibrium stages in both column sections and operating conditions. Equipment duties were computed using the model of Bisgaard et al. (2015). In this work, a reboiler and a condenser was added to the HIDiC design. In general, reserving some reboiler and condenser duty for control is necessary, though this increases the operational cost.

Table 1. Steady state operating conditions for the HIDiC

Items	Values
No. of stages	$3 + 40 + 40$
Compression ratio	2.55
Feed pressure	1.013 kPa
Pressure drop across trays	0.0035 kPa
Heat exchange area per stage	5 m^2
Feed flow rate	83.3 $mol\,s^{-1}$
Feed composition (benzene/toluene)	0.5 / 0.5 mol %
Top product composition (benzene)	0.995 mol %
Bottoms product composition (benzene)	0.005 mol %
Feed thermal condition (vapour fraction)	0.5
Overall Heat Transfer Coefficient	0.6 $kW\,K^{-1}\,m^{-2}$
Compressor isentropic efficiency	72 %
Height over the weir	1.25
Weir height	0.1 m
Reboiler and condenser time constants†	300 s
Compressor time constant†	10 s
Feed pre-heater duty	500 kW
Reboiler duty	791 kW
Compressor duty	483 kW
Condenser duty	2853 kW
Reflux flow rate	56.2 $mol\,s^{-1}$

†Time constants defined as total holdup divided by the throughput at steady state

3. DESIGN OF A DECENTRALIZED CONTROL SYSTEM

In this section a decentralized control system is designed using the LACEY procedure (Luyben (2012)). The following steady state performance criteria are used to evaluate control configurations:

The Niederlinski index (NI): Must be positive for stable control systems.
The Morari resiliency index (MRI): The larger the magnitude of the MRI index, the more resilient the control structure is.
The condition number (CN): The smaller the magnitude of the CN index, the more robust the control structure is.
The relative gain array (RGA): Positive RGA elements of unity indicate no interaction between control loops and is therefore preferred.

A hierarchical control system is designed consisting of a lower level regulatory control layer with a supervisory control layer on top. The purpose of the regulatory control layer is to stabilize modes which are unstable and slow modes drifting far away from nominal conditions. The purpose of the supervisory control layer is to control primary variables using as manipulated variables the set points of the regulatory control layer and any unused variables. The control system is designed from the bottom and up, starting with the regulatory control layer (Skogestad (2004)).

3.1 Regulatory Control Layer

The variables that must be controlled at the regulatory control layer are determined using engineering judgement and considerations of the conventional distillation column given by Skogestad (2007). The identified controlled variables are given in the following:

- **Liquid levels:** The liquid levels (holdups) in the condenser, reboiler and in the bottom of the rectifying section are integrating modes that must be stabilized.
- **Pressure:** Pressure is a measure of a vapour holdup and its response therefore closely resembles an integrating process. It is proposed to control the pressures of both the rectifying section and the stripping section. This is expected to reduce the effect of disturbances and thus contribute to indirect composition control due to the strong coupling of pressures, temperatures, internal heat transfer and compositions.
- **Temperature:** The benefits of including a fast inner temperature control loop is explained by Skogestad (2007). This is expected to contribute to indirect composition control due to strong coupling of temperature with compositions. One problem of temperature-based column control is pressure variation. In the HIDiC, the pressure difference between the two column sections is used as a driving force for separation. Therefore pressure changes continuously in the HIDiC. Closing a temperature loop including only one temperature measurement is unlikely to give the desired composition control, due to composition being a function of both temperature and pressure. One method that can be used to overcome this challenge is to control a temperature difference between two stages located in either column sections (Luyben (1969); Yu and Luyben (1984)). Skogestad (2007) recommends to control temperature in the column end of the most valuable component, because this minimizes composition variations in the important end. According to ICIS (2015) the price of benzene is 1.04 \$ kg^{-1} and the price of toluene is 0.853 \$ kg^{-1}. Thus, the temperature differential is to be located in the rectifying section. The single most sensitive tray in the rectifying section is determined using criteria proposed by Luyben (2006). For each of the manipulated variables available, a temperature gain matrix is computed from step responses using perturbations of 1 % in manipulated variables. Based

on the slope, sensitivity and singular-value decomposition (SVD) analysis criteria, the most sensitive tray was determined as number 15. Using a tray at the top of the column where composition is mainly one component, the temperature differential to be controlled is $\Delta T = T_2 - T_{15}$.

The liquid levels are paired using the pair close rule of Minasidis et al. (2015). The suggested pairings are given by [1]

- $\boldsymbol{L_{\text{int}} \rightarrow M_{\text{int}}}$**:** The liquid level of the bottom of the rectifying section (intermediate holdup) is controlled by manipulating the outlet liquid flow rate of the throttling valve. In this work, this level is assumed perfectly controlled.
- $\boldsymbol{D \rightarrow M_{\text{Cnd}}}$**:** The distillate flow rate is used to control the liquid level in the condenser.
- $\boldsymbol{B \rightarrow M_{\text{Rbl}}}$**:** The bottoms flow rate is used to control the liquid level in the reboiler.

The remaining three controlled variables P_{R}, P_{S} and ΔT are the pressure in both column sections and the temperature differential, respectively. The remaining manipulated variables Q_{F}, Q_{Rbl}, Q_{Cnd}, E and L are the feed pre-heater, reboiler, condenser and compressor duties and the reflux flow rate, respectively. Thus, there are a total of $\binom{5}{3} = 10$ possible control configurations. The performance criteria for each configuration are given in Table 2. The NI is negative for configuration 1, 5-6 and 8-9 indicating stability problems, and are therefore rejected. Configurations 2-4 have high CN indicating inefficiency with respect to rejecting external disturbances and are therefore not promising choices either. The remaining configurations are 7 and 10 and both are chosen. The pairing is evaluated using the steady state relative gain array (RGA) elements from the steady state open loop gain matrix $\boldsymbol{G}(s=0)$,

$$[\Delta E, \Delta Q_{\text{Rbl}}, \Delta Q_{\text{Cnd}}]^T = \boldsymbol{G_7}(s)\,[\Delta P_{\text{R}}, \Delta P_{\text{S}}, \Delta(\Delta T)]^T \quad (1)$$

$$[\Delta E, \Delta Q_{\text{F}}, \Delta Q_{\text{Cnd}}]^T = \boldsymbol{G_{10}}(s)\,[\Delta P_{\text{R}}, \Delta P_{\text{S}}, \Delta(\Delta T)]^T \quad (2)$$

The steady state gain matrix is computed from step responses using perturbations in manipulated variables of 1 %. The following steady state relative gain matrices are obtained:

$$\Gamma_{\boldsymbol{G_7}(s)} = \begin{bmatrix} \mathbf{1.5612} & -0.8148 & 0.2536 \\ -0.6020 & \mathbf{1.4394} & 0.1626 \\ 0.0408 & 0.3753 & \mathbf{0.5839} \end{bmatrix} \quad (3)$$

$$\Gamma_{\boldsymbol{G_{10}}(s)} = \begin{bmatrix} \mathbf{1.4869} & -0.8529 & 0.3660 \\ -0.5531 & \mathbf{1.5733} & -0.0202 \\ 0.0662 & 0.2796 & \mathbf{0.6542} \end{bmatrix} \quad (4)$$

The suggested pairing is highlighted in boldface numbers. In the following configuration 7 is denoted the (Q_{Rbl},Q_{Cnd},E)-configuration and 10 is denoted the (Q_{F}, Q_{Cnd},E)-configuration.

3.2 Supervisory Control Layer

Control Configurations In this work, dual composition control is considered. Using the $(Q_{\text{Rbl}}, Q_{\text{Cnd}}, E)$-configuration for regulatory control, there are 6 manipulated variables available Q_F, ΔT_{sp}, $P_{R,sp}$, $P_{S,sp}$, L, $(L/D)_{sp}$. Thus, there exists $\binom{6}{2} - 1 = 14$ possible configurations. The performance criteria for these configurations are given in Table 3. The NI is positive for all configurations, indicating that all configurations may be stable. The MRI and CN indicate that 1, 5 and 10-11 lack the ability

[1] the symbol $\rightarrow$ means "is used to control".

Table 2. Control system configurations for the regulatory control layer

No.	Config.	NI	MRI$\times 10^{-5}$	CN$\times 10^{3}$
1	L, Q_{Rbl}, Q_{Cnd}	−1.29	5.63	148
2	L, Q_{Rbl}, E	0.60	85	10
3	L, Q_{Rbl}, Q_{F}	1.39	6.50	128
4	L, Q_{Cnd}, E	32	81	10
5	L, Q_{Cnd}, Q_{F}	−2.34	12	67
6	L, E, Q_{F}	−36	93	9
7	$\boldsymbol{Q_{\text{Rbl}}}$, $\boldsymbol{Q_{\text{Cnd}}}$, $\boldsymbol{E}$	**1.31**	**87**	**0.10**
8	Q_{Rbl}, Q_{Cnd}, Q_{F}	−0.12	5.88	1.58
9	Q_{Rbl}, E, Q_{F}	−0.18	33	0.28
10	$\boldsymbol{Q_{\text{Cnd}}}$, $\boldsymbol{E}$, $\boldsymbol{Q_{\text{F}}}$	**1.26**	**98**	**0.10**

Table 3. Control system configurations for supervision of the (Q_{Rbl},Q_{Cnd},E)-configuration

No.	Config.	NI	MRI$\times 10^{-5}$	*RGA*	CN
1	$L/D, Q_{\text{F}}$	1.03	1.40	0.97	3771
2	$L/D, \Delta T$	1.37	296	0.73	18
3	$\boldsymbol{L/D, P_{\text{S}}}$	**0.79**	**1497**	**1.27**	**7**
4	$\boldsymbol{L/D, P_{\text{R}}}$	**0.99**	**1497**	**1.01**	**5**
5	L,Q_{F}	1.03	1.40	0.97	87
6	$\boldsymbol{L}$,$\boldsymbol{\Delta T}$	**1.37**	**117**	**0.73**	**3**
7	L,P_{S}	0.79	40	1.27	234
8	L,P_{R}	0.99	59	1.01	98
9	Q_{F},ΔT	0.99	2.50	1.01	121
10	Q_{F},P_{S}	1.14	0.36	0.88	25823
11	Q_{F},P_{R}	3.73	0.06	0.73	80081
12	ΔT,P_{S}	1.08	255	0.93	36
13	ΔT,P_{R}	1.00	239	1.00	21
14	P_{R}, P_{S}	0.95	394	1.05	27

Table 4. Control system configurations for supervision of the (Q_{F},Q_{Cnd},E)-configuration

No.	Config.	NI	MRI$\times 10^{-5}$	*RGA*	CN
15	Q_{Rbl}, L	1.01	2.40	0.99	25
16	$Q_{\text{Rbl}}, L/D$	1.01	2.40	0.99	1040
17	$Q_{\text{Rbl}}, P_{\text{S}}$	1.20	0.25	0.83	48944
18	$Q_{\text{Rbl}}, P_{\text{R}}$	1.13	0.05	0.88	113550
19	$Q_{\text{Rbl}}, \Delta T$	0.99	2.24	1.01	130
20	$V/B, L$	1.01	52	0.99	72
21	$\boldsymbol{V/B, L/D}$	**1.01**	**1985**	**0.99**	**2**
22	$V/B, P_{\text{S}}$	1.19	321	0.84	40
23	$V/B, P_{\text{R}}$	1.14	48	0.88	137
24	$V/B, \Delta T$	0.99	233	1.01	16
25	L, P_{S}	0.95	49	1.05	245
26	L, P_{R}	1.00	52	1.00	103
27	$\boldsymbol{L, \Delta T}$	**1.85**	**56**	**0.54**	**5**
28	$\boldsymbol{L/D, P_{\text{S}}}$	**0.95**	**2005**	**1.05**	**6**
29	$\boldsymbol{L/D, P_{\text{R}}}$	**1.00**	**2047**	**1.00**	**3**
30	$\boldsymbol{L/D, \Delta T}$	**1.85**	**269**	**0.54**	**9**
31	$P_{\text{Str}}, P_{\text{Rec}}$	0.97	348	1.03	38
32	$P_{\text{Str}}, \Delta T$	1.05	247	0.95	49
33	$P_{\text{Rec}}, \Delta T$	1.00	236	1.00	23

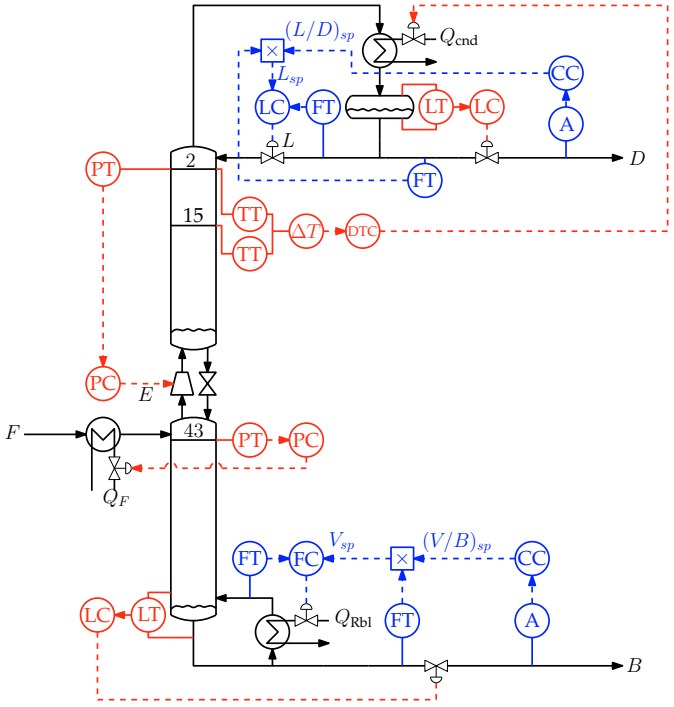

Fig. 2. Fully Decentralized control scheme. Legend: Blue line is supervisory control and red line is regulatory control.

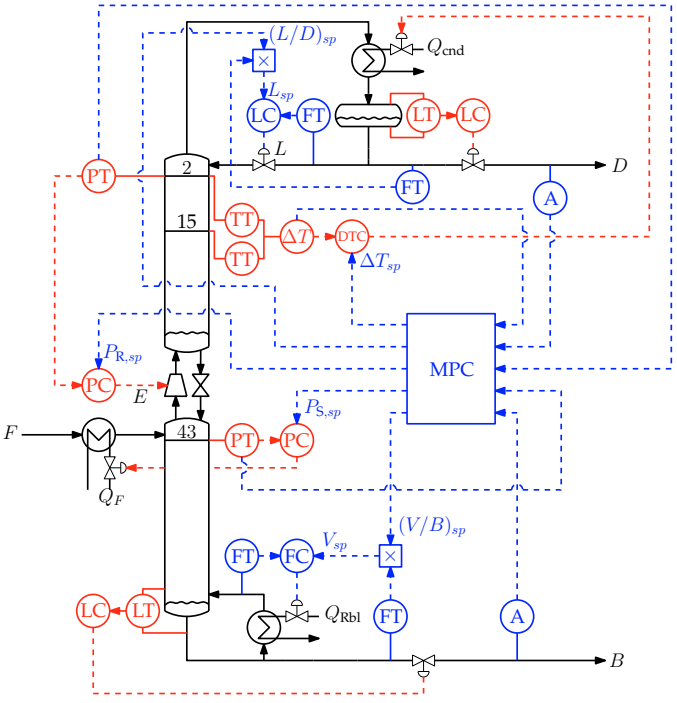

Fig. 3. MPC based supervisory control scheme. Legend: Blue line is supervisory control and red line is regulatory control.

to counteract external disturbances and are therefore not promising. Based on both the CN and MRI, configuration 3-4 and 6 should outperform the rest of the configurations, which are 2, 5, 7-9 and 12-14. Configuration 4 is chosen as the only candidate of these three configurations, since its RGA element is close to unity.

Using the $(Q_{\text{F}}, Q_{\text{Cnd}}, E)$-configuration for regulatory control, there are 7 manipulated variables available L, $(L/D)_{sp}$, Q_{Rbl}, $(V/B)_{sp}$, ΔT_{sp}, $P_{R,sp}$, $P_{S,sp}$. Thus, there exists $\binom{7}{2} - 2 = 19$ possible configurations. The performance criteria for these configurations are given in Table 4. The NI indicates that all the control configurations may be stable. The MRI and CN indicate that configuration 16-18, 23 and 25 will be difficult to operate and are therefore unfavourable. Based on the CN and MRI, configuration 21 and 27-30 should outperform the rest of the configurations, which are 15, 19-20, 22-24, 26 and 31-33. These five remaining configurations have been highlighted using boldface. The MRI of configuration 27 and 30 is about 50 times and 10 times lower compared to configuration 21 and 28-27, respectively. Furthermore, for both configurations, the RGA elements have a value of about 0.6 indicating severe loop interaction. Thus, these two configurations are not chosen. From the remaining three configurations, 21 and 29 are chosen.

Dynamic Evaluation To determine the best configuration among the three configurations chosen, closed-loop simulations are conducted. The single-input single-output (SISO) PI-controllers were tuned using Skogestad (2003) internal model control (SIMC). Controller tuning was based on sequentially closing and tuning one loop at a time, starting with the fastest loop. First order plus time delay models were obtained from step responses using Skogestads (2003) half-rule for model reduction. At the supervisory control layer, the top composition loop was designed first. Then the bottoms composition loop was designed and detuned until loop interaction was minimal with the top composition loop. The control configurations are exposed to the following disturbance scenario:

- $\boldsymbol{t \geq 0}$**:** +20 % in F.
- $\boldsymbol{t \geq 20h}$**:** +10 % in z_F.
- $\boldsymbol{t \geq 40h}$**:** +10 % in P_F.
- $\boldsymbol{t \geq 60h}$**:** Increase x_D from 0.995 to 0.996
- $\boldsymbol{t \geq 80h}$**:** Increase x_B from 0.005 to 0.006

Figure 4 shows the response of the HIDiC after the system has been subjected to the disturbance scenario. Configuration 21 appears to be the best. Configuration 29 is the second best, and configuration 4 is the worst. Nakaiwa et al. (1999) also demonstrated that a double ratio control scheme is the best for operation of the HIDiC. They did, however not include all loops as has been done here. Configuration 21 is benchmarked against an MPC-based solution in the next section. The process diagram of configuration 21 is shown in Figure 2.

4. SUPERVISORY CONTROL BASED ON MODEL PREDICTIVE CONTROL

Although PI-controllers may be used for supervisory control as cascade controllers, one limitation is that decoupled SISO PI-controllers do not effectively handle interactions among loops. Furthermore, it is difficult to handle process constraints using PI-controllers. Loop interaction was observed between all loops in the decentralized control configuration. Therefore, the MPC needs to coordinate all loops in order to fully realize its poten-

tial. That is, control $CVs = [\, x_D \;\; x_B \;\; P_R \;\; P_S \;\; \Delta T \,]$ using $MVs = [\, (L/D)_{sp} \;\; (V/B)_{sp} \;\; P_{R,sp} \;\; P_{S,sp} \;\; \Delta T_{sp} \,]$. Weights on outputs are $W_{CVs} = [\, 1 \;\; 1 \;\; 0 \;\; 0 \;\; 0 \,]$, since only compositions are important. The compositions were constrained between 0 and 1 to respect physical limitations while the rest of the outputs were unconstrained. Weights on inputs are $W_{MVs} = [\, 0 \;\; 0 \;\; 0 \;\; 0 \;\; 0 \,]$ and weights on input movement rate are $W_{MVs,rate} = [\, 100 \;\; 100 \;\; 3 \;\; 3 \;\; 3 \,]$. The inputs and input movement rates were constrained such that local PI-controllers did not saturate. In the MPC algorithm, the inputs and outputs were scaled using appropriate scaling factors. The sample time of the MPC was 3 minutes, and a prediction horizon of 300 and a control horizon of 5 were chosen. The MPC was implemented using the simulink MPC-toolbox. The linear model used has been obtained from step responses using perturbations of 1 % in manipulated variables. Transfer functions were fitted to these responses and realized into a state-space form representation using a balanced realization. In order to give a fair comparison with the decentralized scheme, the supervisory PI-controllers were digitalized with a sample time of 3 minutes. A backward Euler method was used to compute the integral of the control error in the digital PI-controllers.

Table 5. Integral absolute errors.

	Configuration	
Variable	MPC	PI
x_D	0.0089	0.0163
x_B	0.0141	0.0605

4.1 Dynamic Evaluation

Figure 5 gives the responses of the centralized and the decentralized control systems. In the decentralized control system, the bottoms composition loop was designed last, indicating a loss in performance due to poor handling of interactions. Therefore, the MPC-solution has the largest improvements for control of the bottoms composition. From Table 5 the integral absolute error (IAE) has been reduced with a factor of 4. The pressure in both column sections and the temperature differential affect the compositions. The MPC-based solution takes this into account and gives new set points accordingly, whereas in the decentralized system these have nominal set-points throughout the simulation. In the decentralized system the top composition loop was designed first, therefore the MPC-based solution provides less improvement in control of the top composition. From Table 5 the IAE has been reduced with a factor of 2.

5. CONCLUSIONS

A decentralized control system for the operation of the HIDiC has been designed and benchmarked against a centralized control system based on MPC. The MPC-based solution reduced the IAE of the top and bottoms compositions by a factor of 2 and 4, respectively. The HIDiC is an interactive process. Therefore, multivariable control strategies can provide better control performance.

REFERENCES

Bisgaard, T., Huusom, J., and Abildskov, J. (2015). Modeling and analysis of conventional and heat-integrated distillation columns. *Aiche Journal*, 61(12), 4251–4263.

Bisgaard, T., Huusom, J., and Abildskov, J. (2017). Optimal operation and stabilising control of the concentric heat-integrated distillation column (HIDiC). *Computers and Chemical Engineering*, 96, 196–211.

Huang, K., Wang, S., Iwakabe, K., Shan, L., and Zhu, Q. (2007). Temperature control of an ideal heat-integrated distillation column (HIDiC). *Chemical Engineering Science*, 62(22), 6486–6491.

Liu, X., Zhou, Y., Cong, L., and Ding, F. (2011). High-purity control of internal thermally coupled distillation columns based on nonlinear wave model. *Journal of Process Control*, 21(6), 920–926.

Luyben, W. (1969). Feedback control of distillation columns by double differential temperature control. *Industrial & Engineering Chemistry Fundamentals*, 8(4), 739–744.

Luyben, W. (2006). Evaluation of criteria for selecting temperature control trays in distillation columns. *Journal of Process Control*, 16(2), 115–134.

Luyben, W. (2012). *Practical distillation control*. Springer Science & Business Media.

Mah, R., Nicholas, J., and Wodnik, R. (1977). Distillation with secondary reflux and vaporization: A comparative evaluation. *AIChE Journal*, 23(5), 651–658.

Minasidis, V., Skogestad, S., and Kaistha, N. (2015). Simple rules for economic plantwide control. *Proceedings of PSE2015/ESCAPE25*, 101–108.

Nakaiwa, M., Huang, K., Endo, A., Naito, K., Owa, M., Akiya, T., Nakane, T., and Takamatsu, T. (1999). Evaluating control structures for a general heat integrated distillation column (general HIDiC). *Computers and Chemical Engineering*, 23(1), 851–854.

Nakaiwa, M., Huang, K., Owa, M., Akiya, T., Nakane, T., and Takamatsu, T. (1998). Operating an ideal heat integrated distillation column with different control algorithms. *Computers and Chemical Engineering*, 22(1), 389–393.

Schmal, J., Kooi, H.V.D., Rijke, A.D., Ž. Olujic, and Jansens, P. (2006). Internal versus external heat integration: Operational and economic analysis. *Chemical Engineering Research and Design*, 84(5), 374–380.

Shahandeh, H., Ivakpour, J., and Kasiri, N. (2014). Feasibility study of heat-integrated distillation columns using rigorous optimization. *Energy*, 74, 662–674.

Skogestad, S. (2003). Simple analytic rules for model reduction and pid controller tuning. *Journal of Process Control*, 13(4), 291–309.

Skogestad, S. (2004). Control structure design for complete chemical plants. *Computers and Chemical Engineering*, 28(1–2), 217–234.

Skogestad, S. (2007). The dos and don'ts of distillation column control. *Chemical Engineering Research and Design*, 85(A1), 13–23.

Yu, C. and Luyben, W. (1984). Use of multiple temperatures for the control of multicomponent distillation columns. *Industrial & Engineering Chemistry Process Design and Development*, 23(3), 590–597.

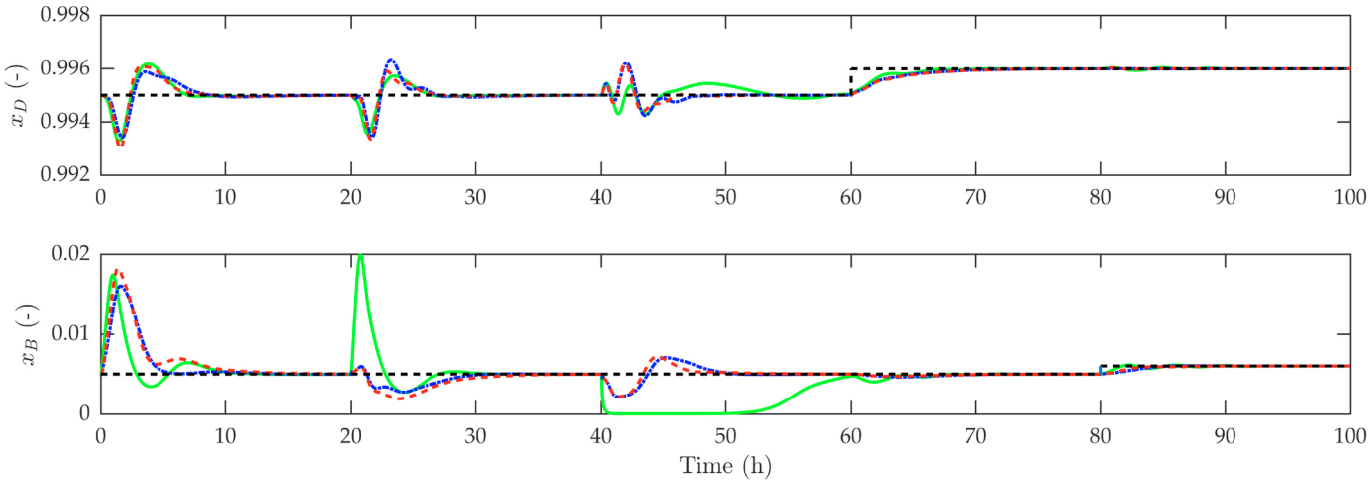

Fig. 4. Composition response of the HIDiC. Legend: The green line is configuration 4, the blue line is 21 and the red line is 29.

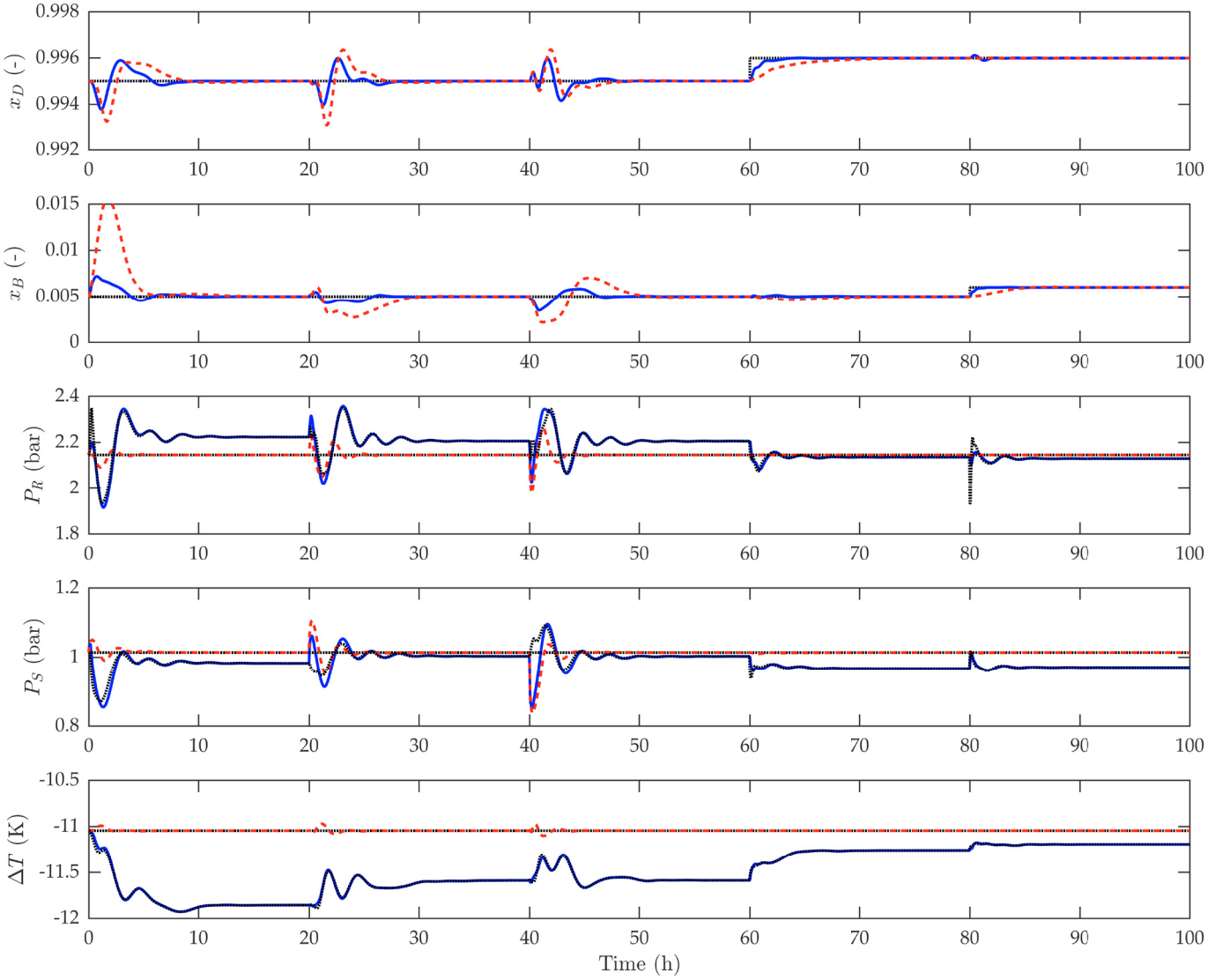

Fig. 5. MPC vs PI. Legend: The blue line is MPC response, the red dashed line is PI response and the black dotted line is setpoints.